



LIBRARY  
AERONAUTICAL RESEARCH COUNCIL  
1967

MINISTRY OF AVIATION  
AERONAUTICAL RESEARCH COUNCIL  
CURRENT PAPERS

The Interaction of the Reflected Shock with the  
Boundary Layer in a Shock Tube and its  
Influence on the Duration of Hot Flow in the  
Reflected-Shock Tunnel. Part II

By

*L. Davies, Ph.D., A.Inst.P.*

LONDON: HER MAJESTY'S STATIONERY OFFICE

1967

Price 5s. 6d. net



The Interaction of the Reflected Shock with the Boundary  
Layer in a Shock Tube and its Influence on the Duration of  
Hot Flow in the Reflected-Shock Tunnel. Part II

- By -

L. Davies, Ph.D., A.Inst.P.

---

PART II\* Calculations for argon, nitrogen, and carbon dioxide with hydrogen  
or helium as driver gases.

Contents

	<u>Page</u>
Introduction .. .. .	3
Theory .. .. .	3
1. Nitrogen .. .. .	5
2. Argon .. .. .	6
3. Carbon Dioxide .. .. .	8
4. Discussion on the results of the calculations and the experiment to differentiate between the effects of transmitted-shock bifurcation and instability of the contact surface on cooling at the end plate .. .. .	8

---

-----  
\*Part II replaces N.P.L. Report 1167 - A.R.C.27 210

Part I A.R.C. C.P. No.880

Nomenclature

a	sound speed
$A_{ij}$	$a_i/a_j$
L	length of shock tube low pressure section
M	Mach number ( $M_1$ = Primary shock Mach number)
p	pressure
$P_{ij}$	$p_i/p_j$
t	time
U	shock velocity
u	flow velocity
$U_{ij}$	$u_i/a_j$
x	distance
$\rho$	density
$\gamma$	specific heat ratio = $C_p/C_v$ (in usual terminology)
$\alpha_i$	$\frac{\gamma_i + 1}{\gamma_i - 1}$
$\beta_i$	$\frac{\gamma_i - 1}{2\gamma_i}$
$\delta_i$	$\sqrt{\frac{2}{\gamma_i (\gamma_i - 1)}}$

Subscripts

1	Initial conditions in test gas
2	Flow behind primary shock
3	Expanded high pressure driver gas region
4	Initial conditions in driver gas
5	Flow behind reflected shock
7	Flow behind transmitted shock
St.bl.	Stagnation conditions in boundary layer flow

Note

Parameters which are marked thus .....  $M_{b1}^*$  refer to the case where the transmitted shock is interacting with the boundary layer.

Parameters which are starred thus .....  $U_7^*$  refer to the flow which emerges through the rear limbs (AB see Fig.1) of the bifurcated foot.

## Introduction

Using the theory outlined in Part (I) calculations of the pressure rise through the transmitted shock of the contact surface and reflected shock interaction in a shock tube, and the total pressure in the boundary-layer gas are presented. The test gases are argon, nitrogen and carbon dioxide, and the driver gases are helium and hydrogen.

Experimental evidence in the form of Schlieren photographs is presented for nitrogen and argon.

It appears that if hydrogen is used as driver gas and argon as test gas then there is the possibility of observing the cooling of the hot reservoir gas near the end plate by means of interface instability without the influence of shock bifurcation cooling.

## Theory

In Part I of this paper it was shown that using the rather crude concept of a boundary layer consisting of a layer of gas of unspecified thickness having wall temperature and velocity, a reasonably good description of the interaction of the reflected and transmitted shock waves with the boundary layer could be obtained. This model was first developed for shock-tube application by Mark<sup>2</sup>. The disadvantages of this model are that the boundary-layer thermal and velocity gradients are not taken into account, neither is there any consideration of the manner in which the stagnant boundary-layer gas adjusts to the higher pressure downstream of the shock or of the interaction of the two streams emerging through the normal and oblique shock systems (see Fig.1). Even so it is considered that the useful description of the phenomena obtained using this simplified approach justifies its application to this problem.

On the basis of this model, and using shock-fixed co-ordinates, it is considered that when the stagnation pressure of the boundary-layer gas is less than the pressure behind the normal shock the resulting accumulation of this gas (unable to enter the region behind the shock), gives rise to the familiar bifurcated shock formation at the intersection of the shock with the tube wall. A consequence of this is that the gas which emerges through the two oblique shocks (see Fig.1) has a higher velocity relative to the normal shock than the flow which emerges through the normal shock. Applying this to the reflected shock in laboratory co-ordinates (as opposed to shock-fixed co-ordinates) the flow which emerges through the normal shock is stationary whereas the flow which emerges through the oblique shocks moves towards the end wall. When the transmitted shock is bifurcated, cold gas flow through the oblique shocks provides a means for the early arrival of cold gas at the end plate.

In order to calculate the angles in the oblique shock system which constitutes the bifurcated foot, and to calculate the emergent gas velocity the following formulae may be used. (See Part I, for their derivation.)

The/

The boundary layer stagnation pressure is given by

$$\frac{P_{st.bl}}{P_i} = \frac{\left[ \frac{(\gamma_{bl} + 1)}{2} M_{bl}^2 \right] \frac{\gamma_{bl}}{\gamma_{bl}^{-1}}}{\left[ \frac{2\gamma_{bl}}{(\gamma_{bl} + 1)} M_{bl}^2 - \left( \frac{\gamma_{bl} + 1}{\gamma_{bl} + 1} \right) \right] \frac{1}{\gamma_{bl}^{-1}}}$$

(See Fig.1).  $\gamma_{bl}$  in all cases will be the specific heat ratio of the test gas (see Part I).

Where

$$M_{bl} = \frac{2M_1^2 (\gamma_1 - 1) - (\gamma_1 - 3)}{(\gamma_1 + 1) M_1} \dots\dots \text{for the reflected shock}$$

$$M_{bl} = a_{31} \left[ \frac{(P_{73} + \alpha_3)}{\delta_3 \gamma_3 (\alpha_3 P_{73} + 1)^{\frac{1}{2}}} + \frac{2a_{53}}{(\gamma_1 - 1)} \left( 1 - P_{65}^{\beta_1} \right) \right]$$

.... for the under-tailored transmitted shock.

$$M_{bl} = a_{31} \left[ \frac{P_{73} + \alpha_3}{\delta_3 \gamma_3 (\alpha_3 P_{73} + 1)^{\frac{1}{2}}} - \frac{a_{53} \delta_1 (P_{65} - 1)}{(\alpha_1 P_{65} + 1)^{\frac{1}{2}}} \right]$$

... for the over-tailored transmitted shock

then the angles COA and COB may be obtained from

$$M^2 \sin^2(\text{COA}) = \frac{(\gamma_1 + 1) \frac{P_{st.bl}}{P_i} + (\gamma - 1)}{2\gamma_1}$$

and

$$\frac{\tan(\text{COA} - \text{COB})}{\tan \text{COA}} = \frac{(\gamma_1 - 1) M_1^2 \sin^2 \text{COA} + 2}{(\gamma_1 + 1) M_1^2 \sin^2 \text{COA}}$$

where

$$M_i = \left[ \frac{2\gamma_1 M^2 - (\gamma_1 - 1)}{(\gamma_1 - 1) M_1^2 + 2} \right]^{\frac{1}{2}} \dots\dots \text{for the reflected shock}$$

and

$$M_i = \left[ \frac{\gamma_3 - 1}{2\gamma_3} \left( \alpha_3 P_{73} + 1 \right) \right]^{\frac{1}{2}} \dots \text{for the transmitted shock.}$$

$M_x$  which is the flow Mach number within the triangle OAB is obtained from

$$M_x^2 \sin^2(\text{COA} - \text{COB}) = \frac{(\gamma_i - 1) \frac{p_{st.bl}}{p_i} + (\gamma_i + 1)}{2\gamma_i \frac{p_{st.bl}}{p_i}}$$

DAB, DAC and the emergent flow Mach number may be obtained using  $(p_j/p_{st.bl})$  values in similar equations.

Values of these parameters for the transmitted shock are calculated and discussed for argon, nitrogen and carbon dioxide in the following sections. Experimental results are compared with theory for nitrogen.

The time of arrival of cold gas at the end plate (which determines the duration of hot flow) is given by

$$t = \frac{LU_s}{(U_s + M_s)} \left(1 - \frac{u_s}{U_s}\right) \left(\frac{1}{U_s} + \frac{1}{(U_7^* \pm U_T)}\right)$$

This formula ignores the effect of secondary waves which are reflected between the contact surface and the end plate. These will have a small effect around the tailoring Mach number but will have increasing effect for large departures from this Mach number.

### 1. Nitrogen

The case where helium is the driver gas has been discussed at length in Part I of this paper. Here further calculations, where hydrogen is the driver gas, will be considered together with some experimental evidence in support of the model.

Using the theory developed in Part I the graphs drawn in Fig.2 have been obtained. Here  $(p'_{st.bl}/p_3)$  (where  $p'_{st.bl}$  is the boundary-layer stagnation pressure in the transmitted shock case) and  $P_{73}$  have been plotted as functions of the Mach number of the primary shock wave.  $(p'_{st.bl}/p_3)$  is seen

to equal  $P_{73}$  at  $M_1 = 5.7$  and value  $\left(\frac{p'_{st.bl}}{p_3}\right) \div P_{73} = 0.8$  is reached at

$M_1 = 6$ , and thus it is for  $M_1 \geq 6$  that bifurcation of the transmitted shock wave becomes significant. It must be remembered, however, that the reflected primary-shock-wave is already bifurcated when it reaches the contact surface, and even if conditions behind the contact surface (i.e., within the expanded driver-gas region) will not support bifurcation of the transmitted shock, it will still require some time interval for the bifurcation effects to disperse. Hence a flow of cold gas to the end plate may be obtained by virtue of the fact that the shock was bifurcated when it encountered the contact surface.

In Fig.3 values of COA' versus  $M_1$  for the transmitted shock are presented and compared with experimental data obtained by Holder, Stuart and North<sup>1</sup>. The simple theory is seen to predict with reasonable accuracy the actual

variation/

relation of COA' with  $M_1$  considering the crudeness of the assumptions on which it is based.

With regard to the cooling of the gas at the end plate a comparison of neutral stability Mach number predictions and bifurcated shock predictions

has been made. In Fig.4 a plot of  $\left(\frac{14T_3}{T_2}\right)$  vs  $M_1$  determines, on using

Markestein's theory, the neutral stability Mach number (see Part I). This

occurs when  $\left(\frac{14T_3}{T_2}\right) = 1$  and this is so for  $M_1 \doteq 6.2$ . Any effects due

to contact surface instability may therefore be expected for  $M_1 \geq 6.2$  as compared to  $M_1 \geq 6.0$  using the bifurcation model.

In Fig.5 details of high pressure and high temperature variation with  $M_1$  for  $H_2 : N_2$  are presented. These were obtained in the N.P.L. 3 in. shock tunnel by Lapworth<sup>5</sup>. Unfortunately only two experimental temperature durations are given in Lapworth's paper and these are shown in Fig.5.

In Fig.6 (a, b, and c) some photographs from the paper by Holder, Stuart and North<sup>1</sup> are reproduced. In Fig.2 it was seen that for  $M_1 < 5.8$  the conditions behind the contact surface, effecting the transmitted shock,

will not support bifurcation, i.e.,  $P_{73} < \frac{P_{st.bl}}{p_3}$ . For  $M_1 > 5.8$  the

conditions will support bifurcation and for  $M_1 = 8$ , for example, strong interaction effects may be expected. In Fig.6(a)  $M_1 = 4$ , and it is clear that the bifurcation of the transmitted shock appears to decrease with time. In Fig.6(b)  $M_1 = 6$  and the transmitted shock interaction is supported and even increases slightly. But in Fig.6(c) at  $M = 8$ , where violent interaction between the transmitted shock and the boundary layer may be expected on the basis of the predictions of Fig.3, extremely strong bifurcation of the transmitted shock is obtained.

Summing up therefore, in the case of hydrogen (as when helium was the driver gas) with nitrogen as channel gas, it appears that the simple theory developed in Part I gives a good description of the bifurcation of the transmitted shock and also the reservoir cooling effects.

## 2. Argon

For primary shock Mach numbers greater than 2.8 Mark has demonstrated that the reflected shock in argon does not bifurcate. However, it will be shown that the transmitted shock does not become bifurcated until  $M_1 = 4.3$  for a helium driver and  $M_1 = 7.5$  for a hydrogen driver. For increasing Mach numbers in these two cases, the bifurcation of the transmitted shock becomes increasingly strong.

In Fig.7 values of  $P_{73}$  and  $(p'_{st.bl}/p_3)$  are plotted as functions of primary shock Mach number for helium as driver gas. As in the nitrogen case, for  $M_1 < 4.06$  the conditions behind the contact surface will not support bifurcation, and since the reflected shock is not bifurcated the reflected and

transmitted/



transmitted shocks behave - in this respect - as suggested by ideal theory. However, for  $M_1 > 4.3$ ,  $p'_{st.bl}/p_7 < 0.8$  and according to Mark when this is the case bifurcation will occur. Therefore for  $M_1 > 4.3$  the transmitted shock should be bifurcated and a flow of cold gas near the walls of the tube directed towards the end plate by means of the mechanism outlined in Part I should occur. Hence cooling due to this effect should be evident for  $M_1 > 4.3$ .

In Fig.8(a) the neutral stability Mach number ( $M_{NS}$ ) is determined as for nitrogen. In this case this Mach number is 3.85 and hence cooling due to interface instability should occur for  $M_1 > 3.85$ .

Here then is a possible means of separating the two effects, for if cooling occurs below  $M_1 = 4.3$  then the interface instability mechanism must be considered as a cause of cooling, but if cooling does not occur until  $M_1 > 4.3$  then this would tend to weaken the case for interface instability. This point is discussed further for a hydrogen driver gas.

$P_{7s}$  and  $(p'_{st.bl}/p_s)$  are plotted in Fig.9 as a function of primary shock Mach number where the driver gas is hydrogen. For  $M_1 < 7$  the region behind the contact surface will not support bifurcation, but for  $M > 7.5$  the transmitted shock will be bifurcated, according to the simple theory. The neutral stability Mach number is obtained for hydrogen driver in Fig.10 and found to be  $M_1 = 5.8$ . Thus for hydrogen as driver gas and argon as driven gas there is a large difference between the neutral stability Mach number (i.e.,  $M_1 = M_{NS} = 5.8$ ), above which cooling of the reservoir gas is expected to occur as a result of interface instability, and the primary shock Mach number ( $M_1 = 7.5$ ) above which bifurcation of the transmitted shock, and the cooling which is suggested to accompany this phenomenon, are to be expected. It is suggested that hydrogen driving into argon is the best case in which to attempt to differentiate between the neutral stability and bifurcation mechanisms for cooling at the end plate in a shock tube.

### Experimental evidence

Some Schlieren photographs taken in the N.P.L. 6 in.  $\times$   $3\frac{1}{2}$  in. shock tube using argon as the test gas and helium as driver gas are presented in Figs.8(b) and 8(c). These pictures give the full field of view.) In Fig.8(b) it is seen that the reflected shock wave remains plain with no bifurcation throughout the Mach number range. Mark<sup>2</sup> had predicted that for  $M_1 > 2.8$  this should be so and Strehlow and Cohen<sup>3</sup> observed this for reflected shocks in argon using streak photography.

In Fig.8(c) the transmitted shock at  $M_1 = 6$  is seen to be bifurcated. This is what would be expected on the basis of the above theory for  $M_1 > 4.3$ . Unfortunately it was impossible to observe the transmitted shock at the lower Mach numbers as the reflected shock interacted with the contact surface upstream of the window section.

From the experimental evidence it is clear that bifurcation of the transmitted shock wave occurs at the higher Mach numbers for helium as driver gas and argon as test gas. A detailed account of these experiments is to be found in Ref.4.

### 3. Carbon Dioxide

Calculations for carbon dioxide were carried out in order to investigate the case of a triatomic gas.

In Fig.11 a plot of  $P_{73}$  and  $(p'_{st.bl}/p_3)$  as functions of primary shock Mach number indicates that below  $M_1 = 7.8$  conditions will not support bifurcation of the transmitted shock. The reflected shock, however, bifurcates most strongly and hence it is to be expected that a gradual dispersion of the bifurcation will occur after the shock passes through the contact surface. Above  $M_1 = 7.8$  bifurcation of the transmitted shock will be supported as  $P_{73}$  then becomes increasingly larger than  $(p'_{st.bl}/p_3)$ . The neutral stability Mach number is seen from Fig.12 to occur at  $M_1 = 8$ . Owing to the very strong interaction between the reflected shock and the boundary layer, however, cooling due to the bifurcation mechanism may occur below the Mach number at which bifurcation of the transmitted shock is supported.

### 4. Discussion on the Results of the Calculations and the Experiment to Differentiate between the Effects of Transmitted-shock Bifurcation and Instability of the Contact Surface on Cooling at the End Plate

The calculations for argon, nitrogen, and carbon dioxide indicate definite regions in the flow in shock tubes. The regions are firstly, those for which bifurcation of the transmitted shock is not supported, i.e., where the stagnation pressure is not less than the pressure behind the transmitted shock, and secondly the region for which bifurcation of the transmitted shock is supported, where the stagnation pressure of the boundary layer fluid is less than the pressure behind the transmitted shock.

Experimental evidence in support of the predictions of the simple model is available for hydrogen as driver gas and nitrogen as driven gas from a paper by Holder, Stuart and North and for argon as test gas with helium as driver gas from reference 4. As a result of the favourable comparison between experiment and theory in both Part I and II it is suggested that this simple theory provides a good description of the bifurcation effect for the transmitted shock in shock tubes. Also the trend of hot flow duration with increasing Mach number predicted by this theory is in fair agreement with experiment.

As a further investigation it is suggested that if hydrogen is used as driver gas and argon as driven gas an observation of the effects of interface instability on reservoir cooling without the effects of transmitted shock bifurcation should be possible, since the neutral stability Mach number corresponds to  $M_1 = 5.8$  whereas bifurcation of the transmitted shock should not occur for  $M_1 < 7.5$ . Table I summarises the conditions under which bifurcation of the transmitted shock becomes significant for various driver-driven gas combinations.

### Acknowledgement

Most of the calculations were carried out by Miss B. Redston.

### References/

References

<u>No.</u>	<u>Author(s)</u>	<u>Title, etc.</u>
1	Holder, D. W. Stuart, C. M. and North, R. J.	The interaction of a reflected shock with the contact surface and boundary layer in a shock tube. A.R.C.22 891. September, 1961.
2	Mark, H.	The interaction of the reflected shock wave with the boundary layer in a shock tube. NACA TM.1418. March, 1958.
3	Strehlow and Cohen	Limitations of the reflected shock technique for studying fast chemical reactions and its application to the observation of relaxation in nitrogen and oxygen. J. Chem. Phys. <u>30</u> , 257, 1959.
4	Davies, L. and Bridgeman, K.	On the interaction of the transmitted shock with the boundary layer in a shock tube using argon as test gas. A.R.C. C.P.879. September, 1965.
5	Lapworth, K. C.	Temperature measurements in a hypersonic shock tunnel. AGARDograph 68, Pergamon Press, 1963. pp.255-269.

---

Table I/

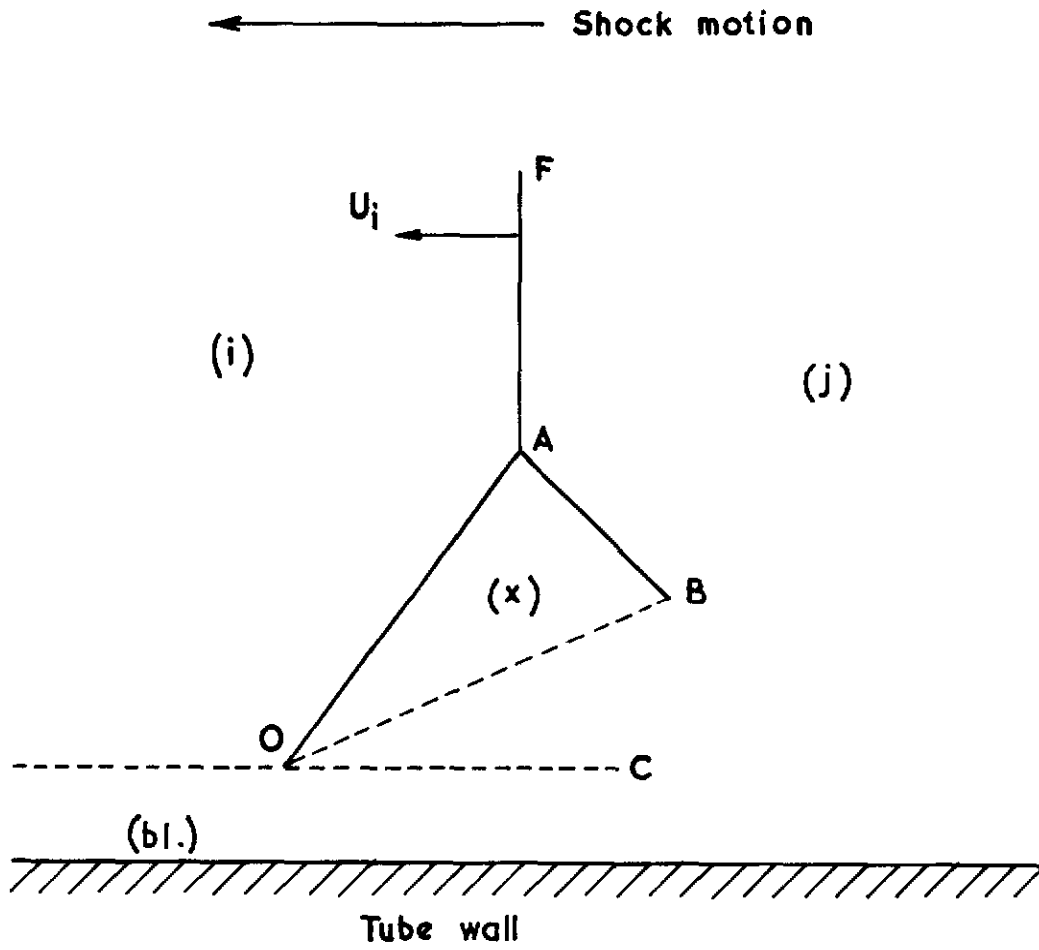
Table I

Driver Gas	Driven Gas	$M_B^*$
Hydrogen	Argon	7.5
	Nitrogen	6
	Carbon Dioxide	7.8
Helium	Argon	4.3
	Nitrogen	3.5

$M_B^*$  = Primary shock Mach number above which bifurcation of the transmitted shock may be expected.

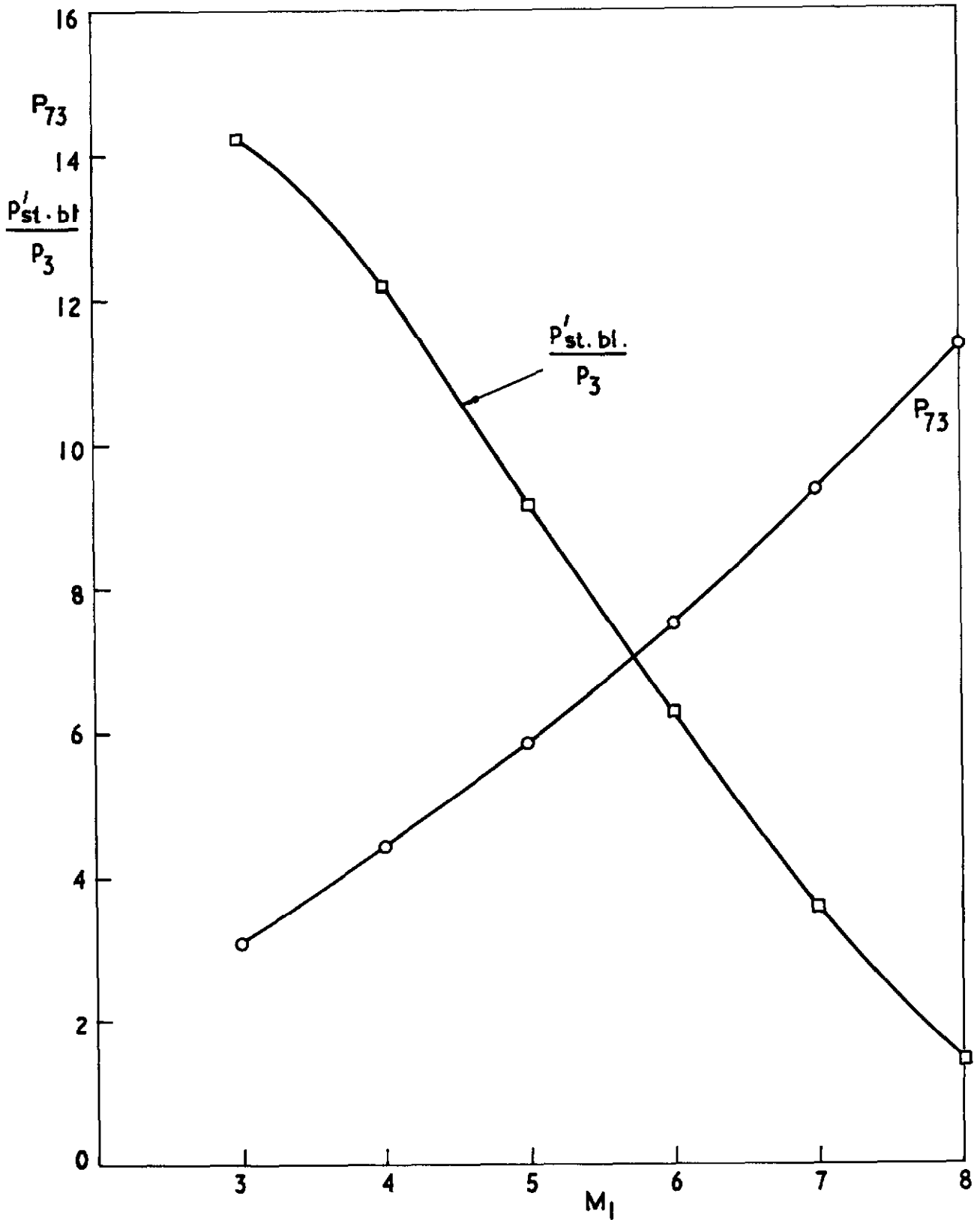
Table showing various primary shock Mach numbers for which transmitted shock bifurcation may be expected using various driver and driven gases.

FIG. 1



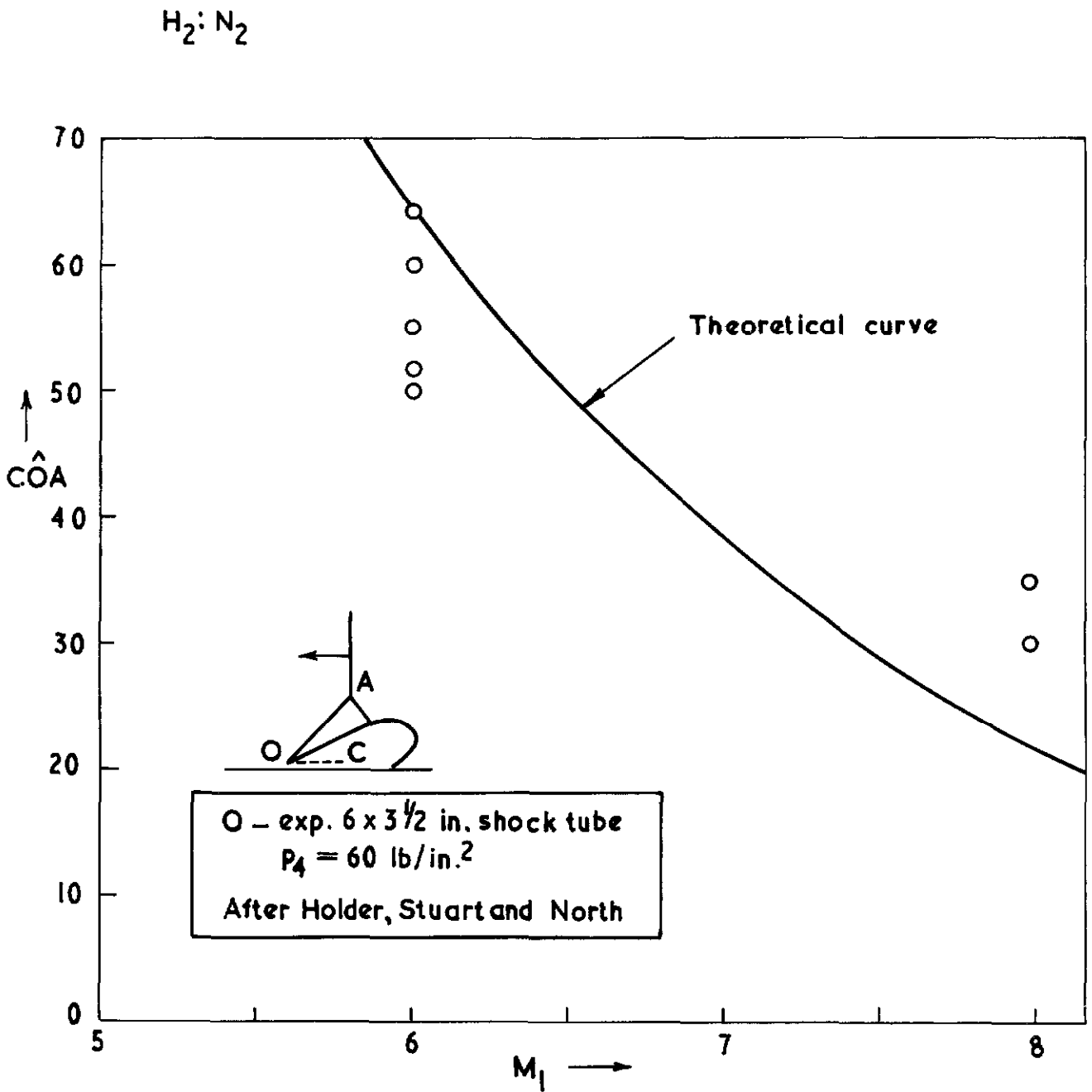
Nomenclature for simple bifurcated shock theory

**FIG. 2**



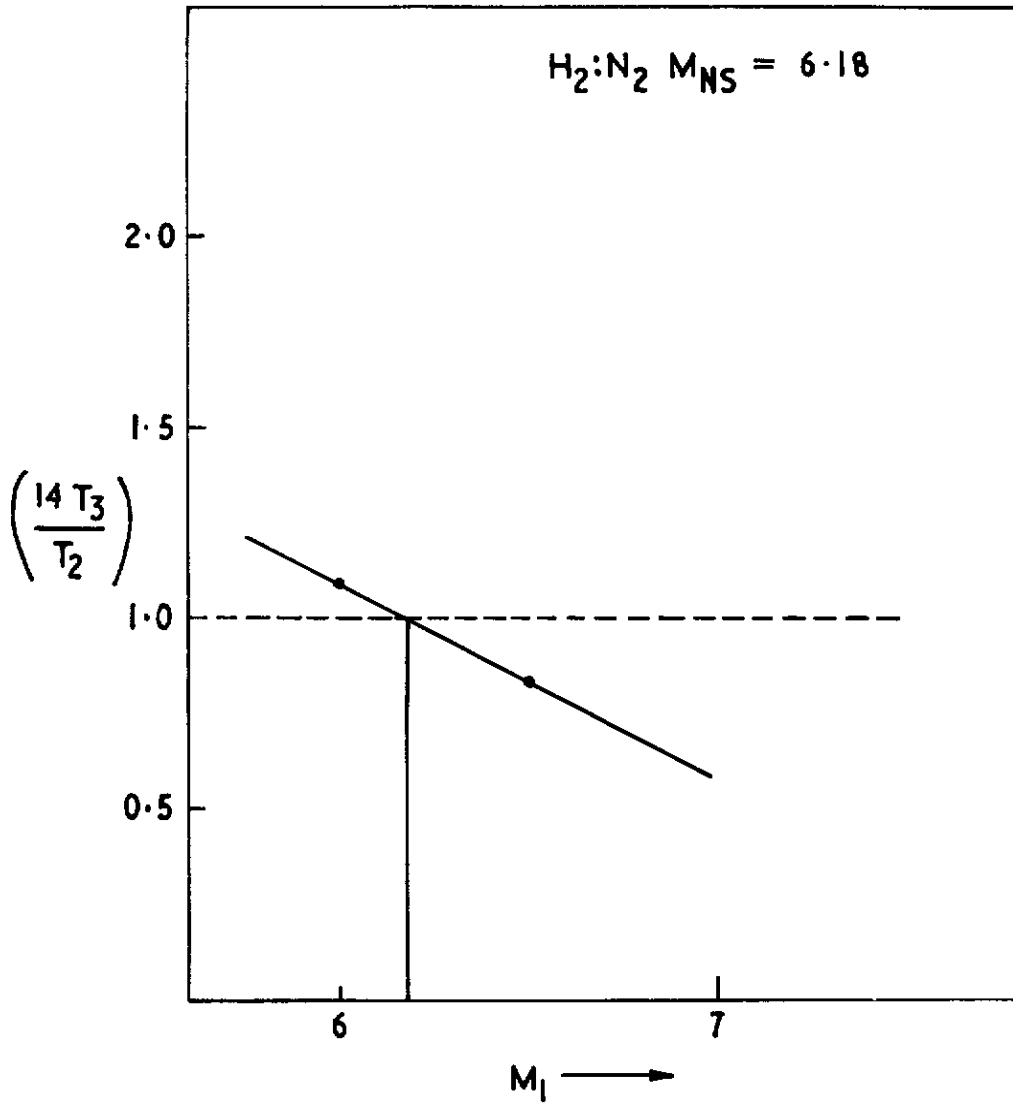
Hydrogen/Nitrogen  $P_{73}$  and  $\frac{P'_{st. bl.}}{P_3}$  vs  $M_1$

**FIG. 3**



Comparison of experimental and theoretical values of  $\hat{C}OA$  for the shock transmitted through a nitrogen → hydrogen interface in a shock tube

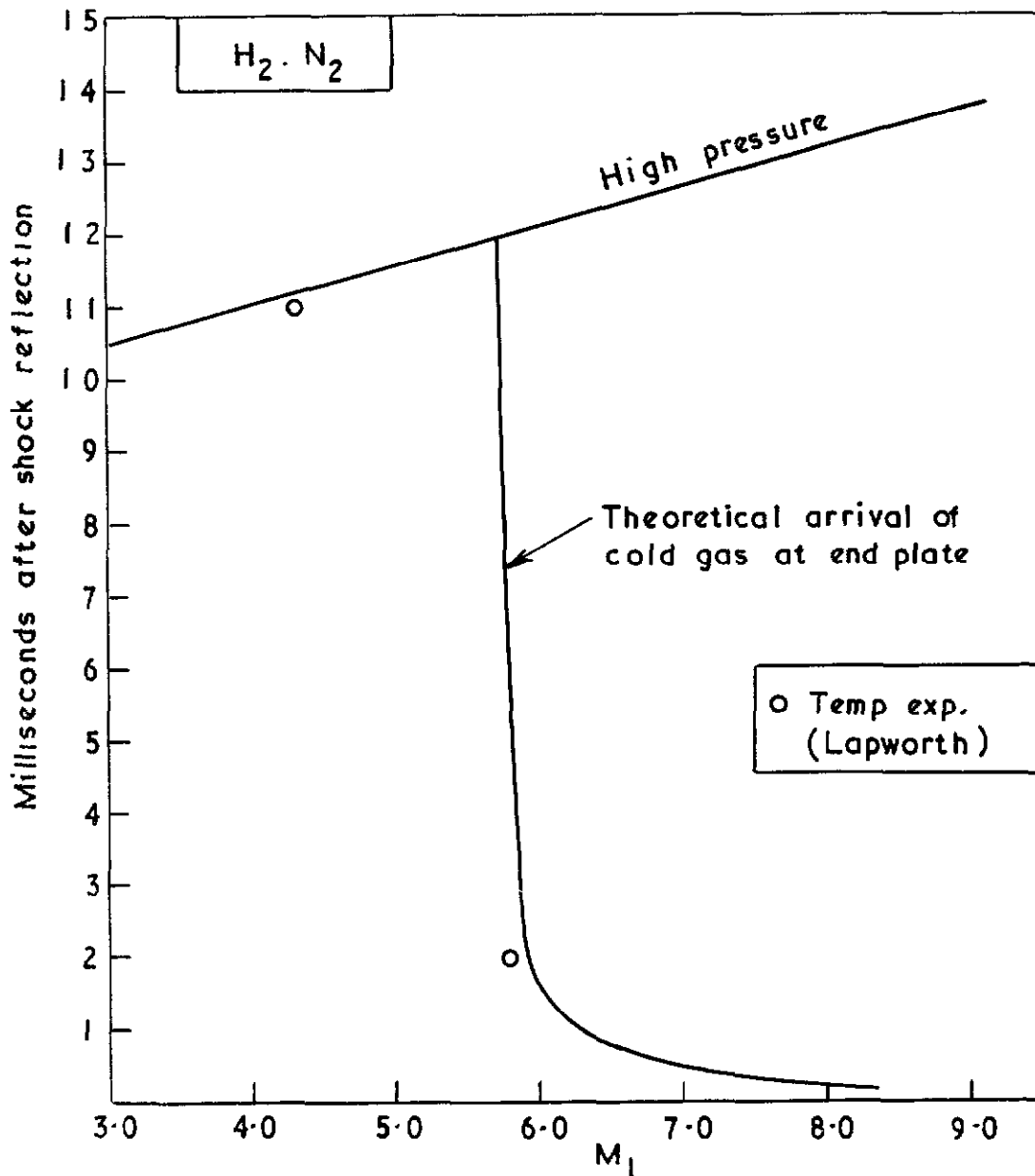
FIG. 4



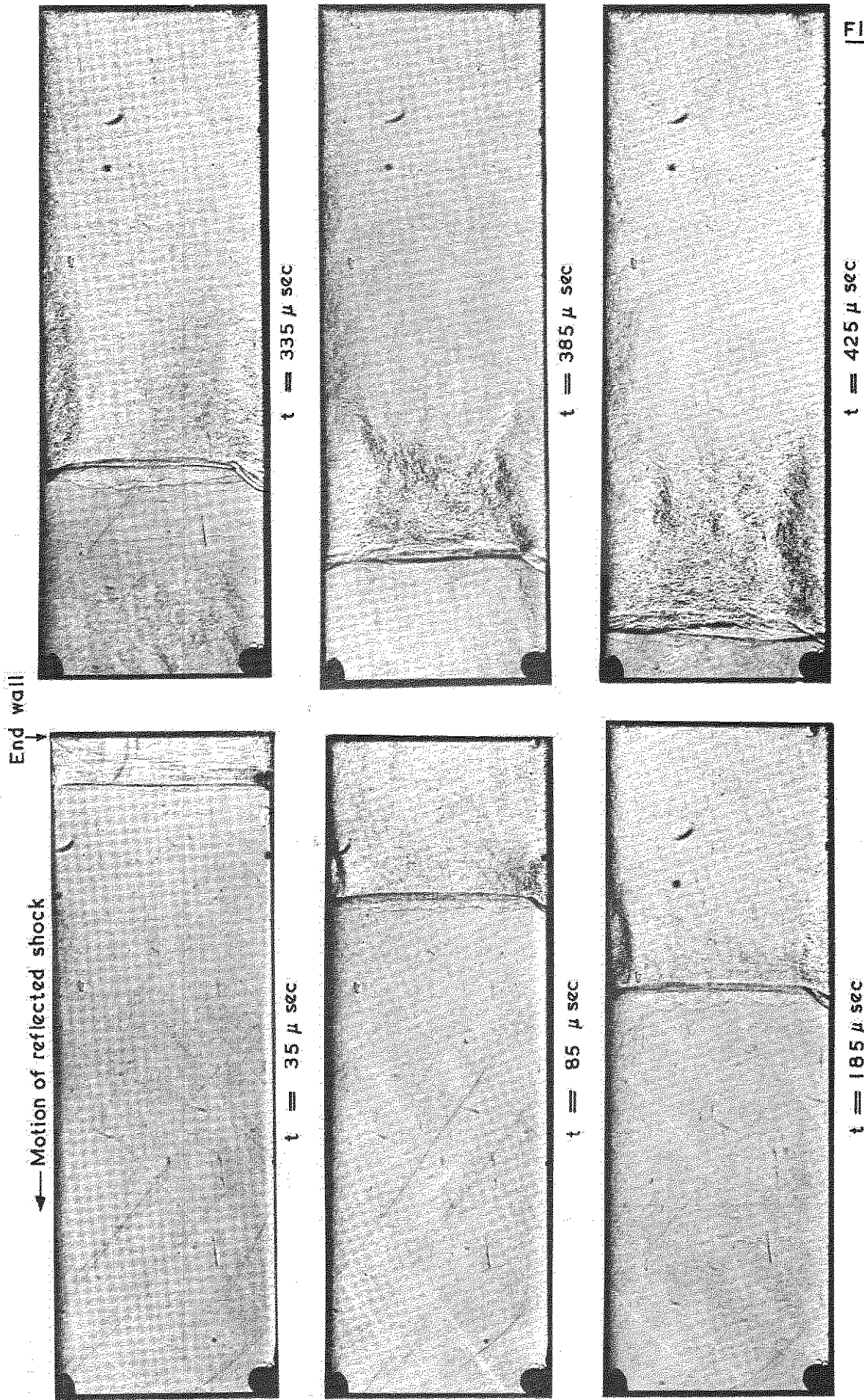
$H_2:N_2$  Neutral stability when  $\frac{14 T_3}{T_2} = 1$



FIG. 5



Duration of high pressure and high temperature in the reservoir of the NPL 3 inch shock tunnel with hydrogen as driven gas and nitrogen as driver gas compared with the theoretical arrival time of cold gas at the end plate



Schlieren photographs of the flow pattern for  $M_1 = 4$ ,  $p_1 = 20 \text{ mm Hg}$   
The times quoted are measured after the reflection of the shock from the end wall  
(After Holder, Stuart and North)

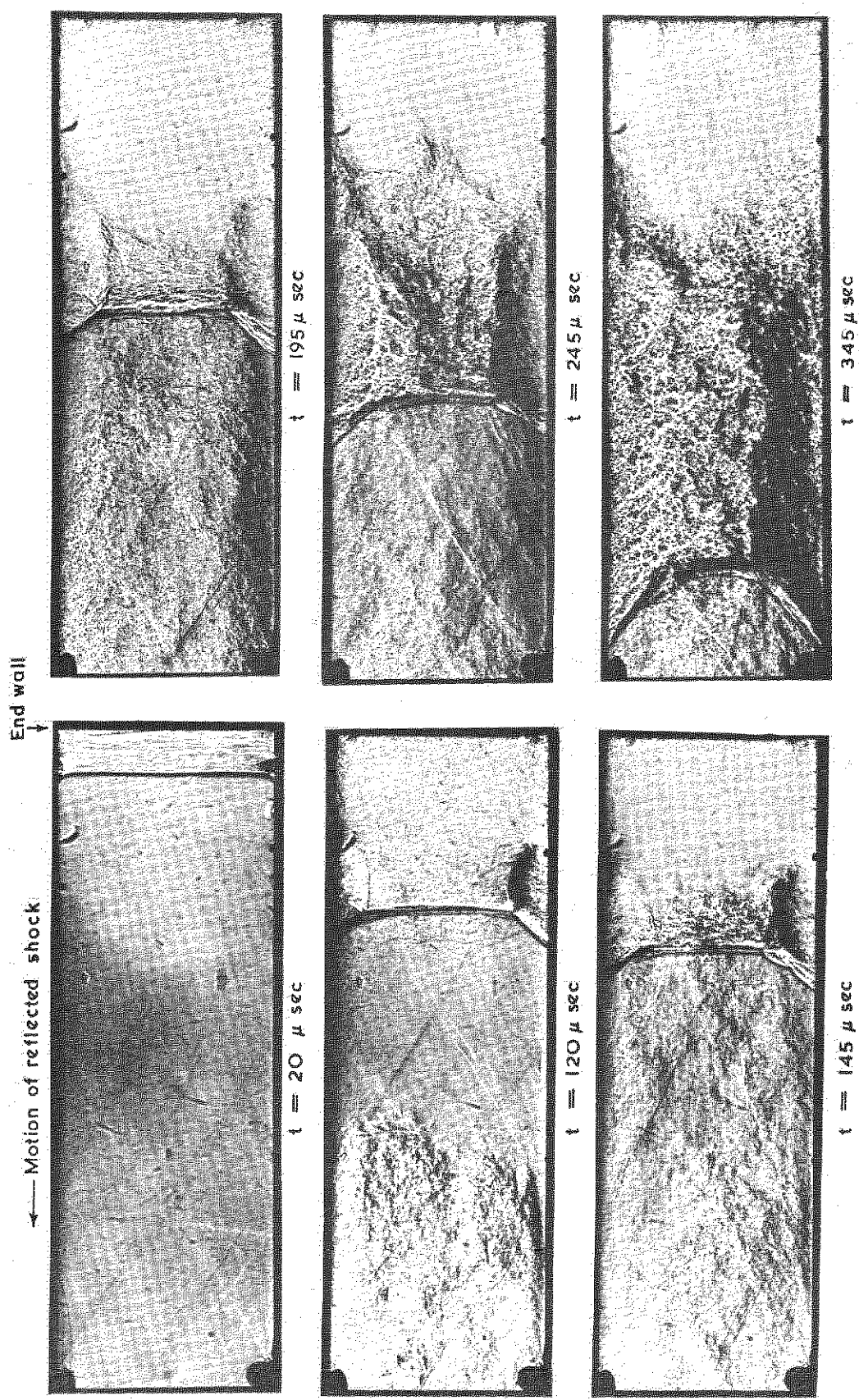
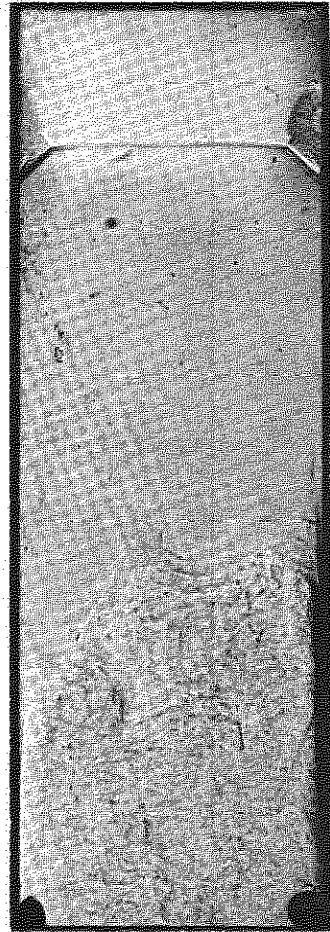


FIG. 6(b)

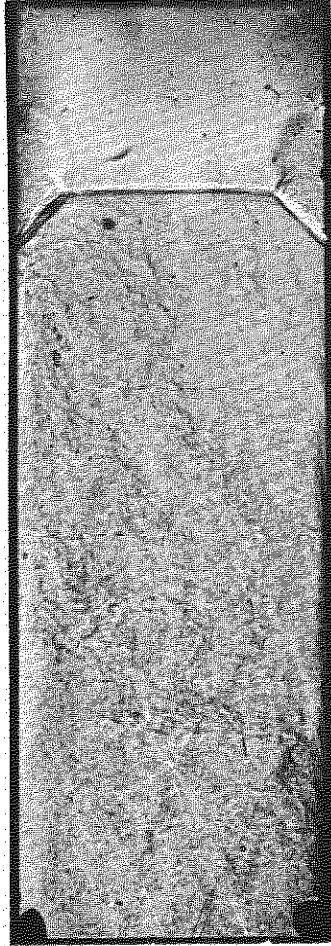
Schlieren photographs of the flow pattern for  $M_1 = 6$ ,  $P_1 = 7$  mm Hg  
The times quoted are measured after the reflection of the shock from the end wall  
(After Holder, Stuart and North)

End wall

← Motion of reflected shock



$t = 50 \mu \text{ sec}$



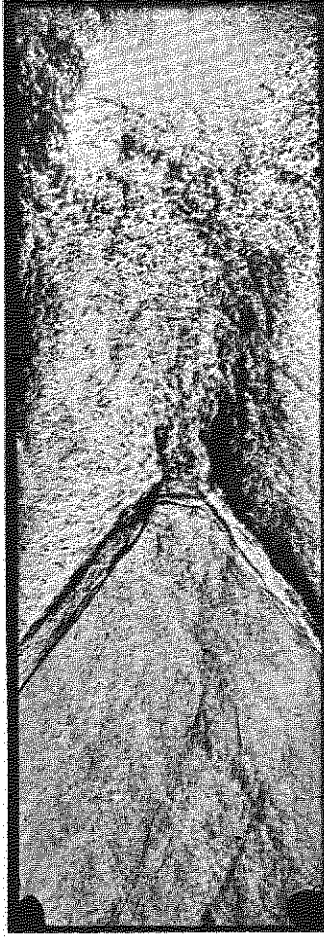
$t = 75 \mu \text{ sec}$



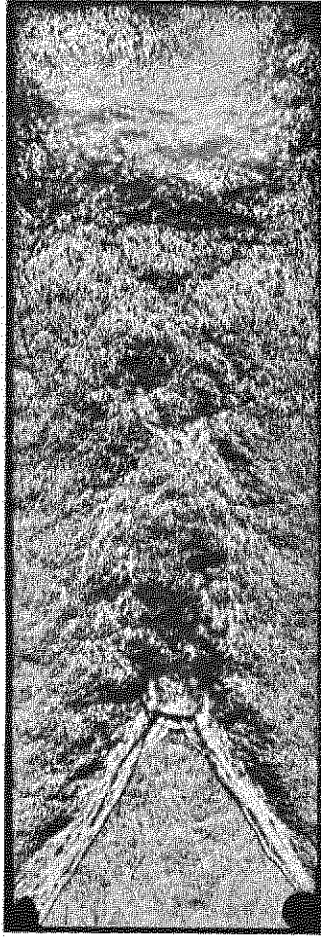
$t = 100 \mu \text{ sec}$



$t = 150 \mu \text{ sec}$



$t = 200 \mu \text{ sec}$

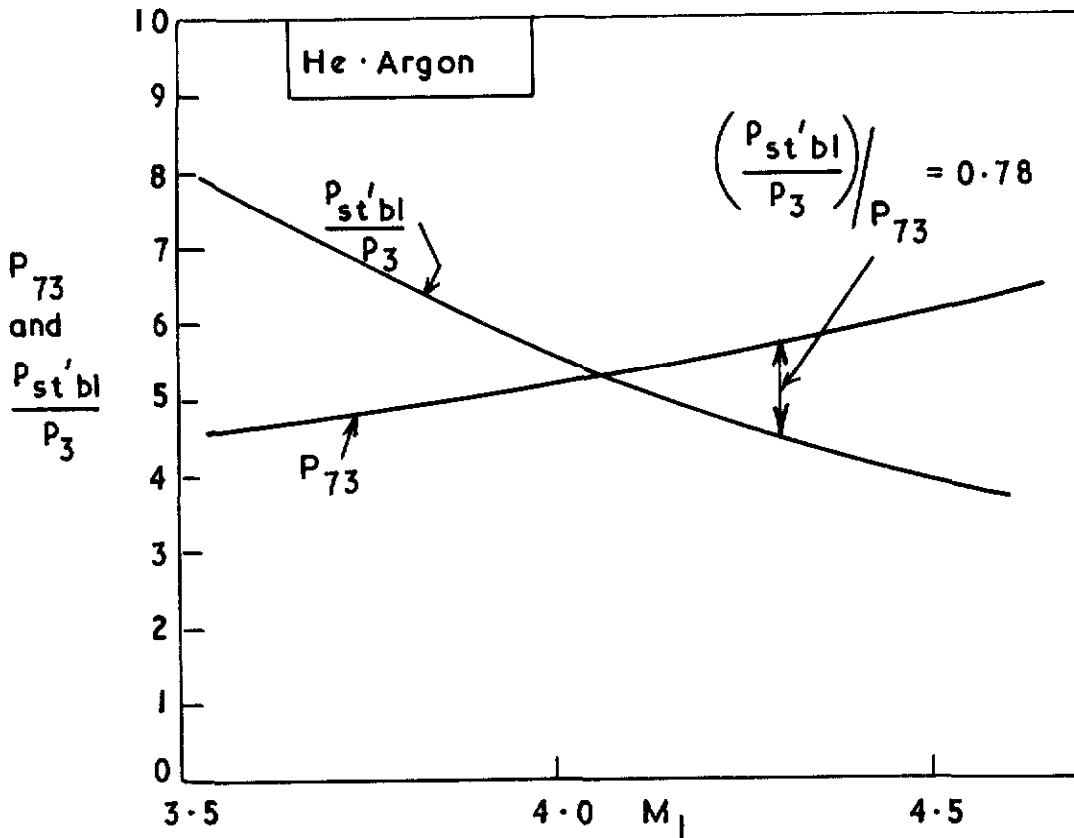


$t = 275 \mu \text{ sec}$

FIG. 6(c)

Schlieren photographs of the flow pattern for  $M_1 = 8$ ,  $p_1 = 2 \text{ mm Hg}$ .  
The times quoted are measured after the reflection of the shock from the end wall  
(After Holder, Stuart and North)

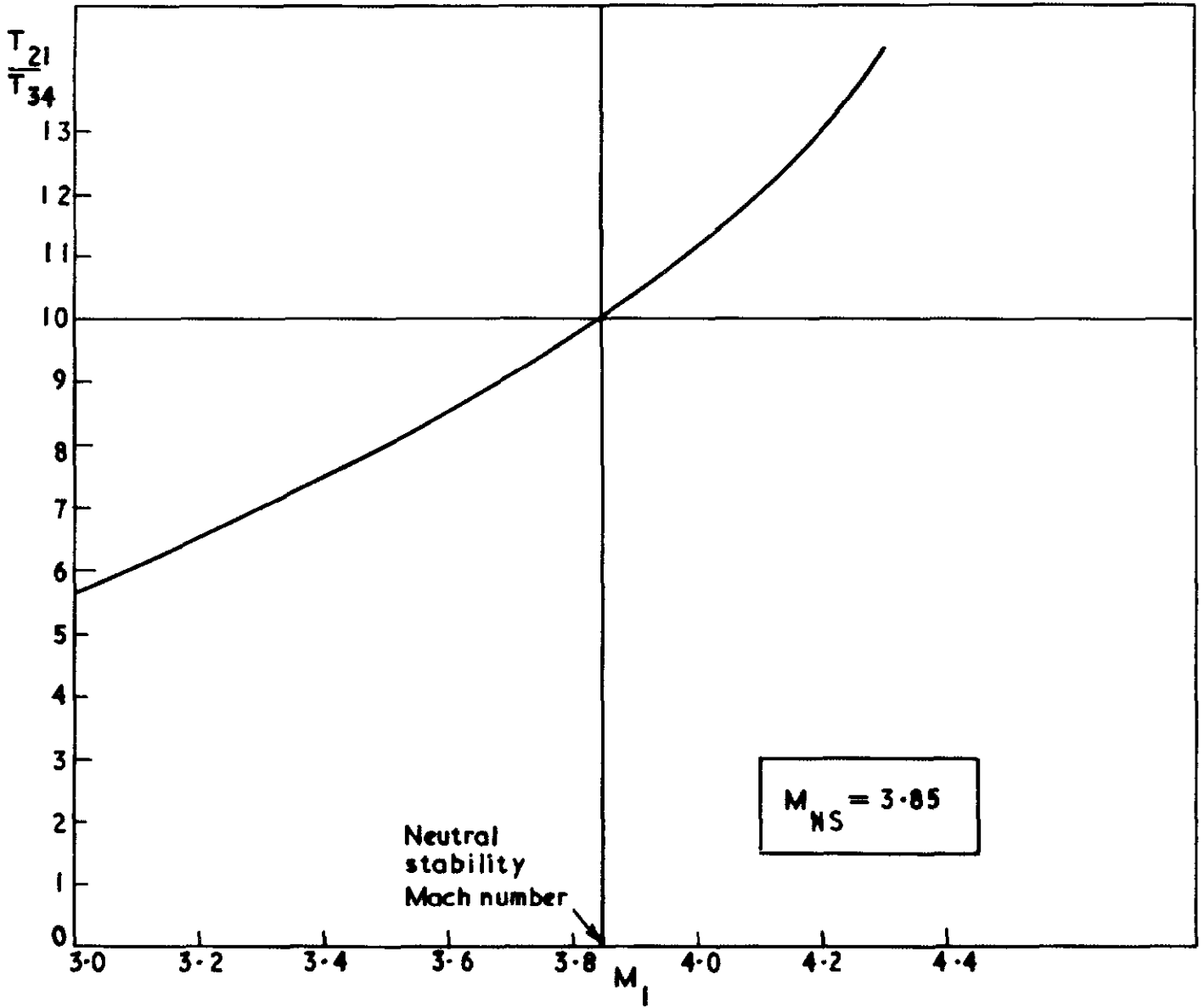
FIG. 7



Plot of  $P_{73}$  and  $\frac{P_{st'bl}}{P_3}$  vs  $M_1$  for He-Argon  
showing that bifurcation may be expected for  
transmitted shock when  $M_1 > 4.3$  i.e.

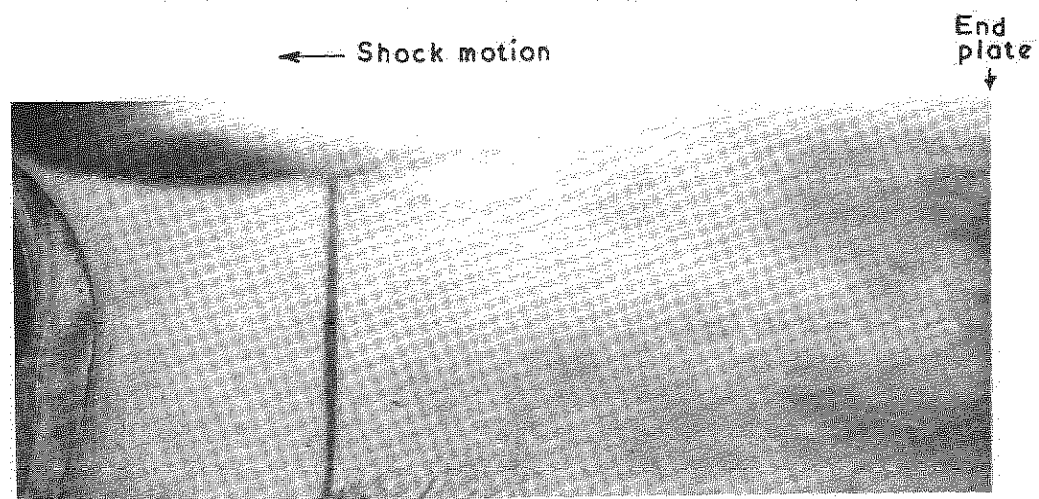
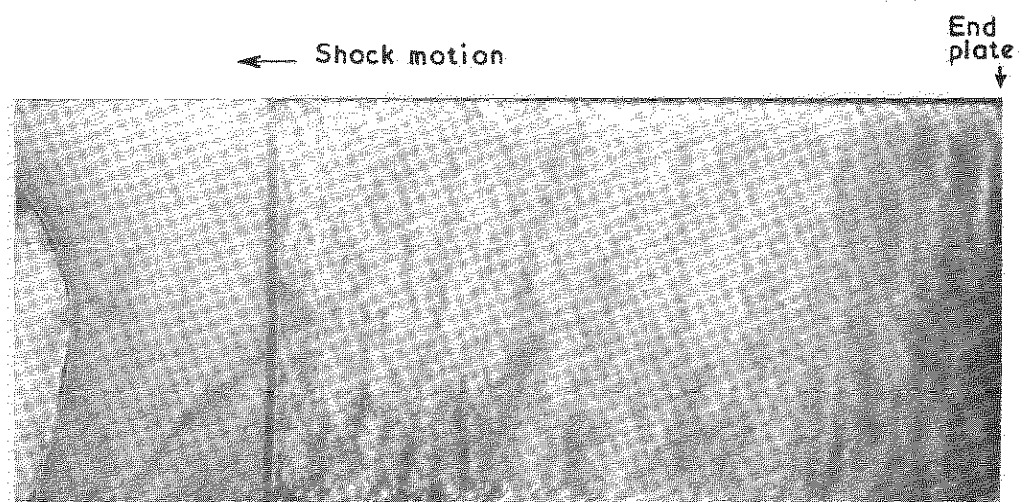
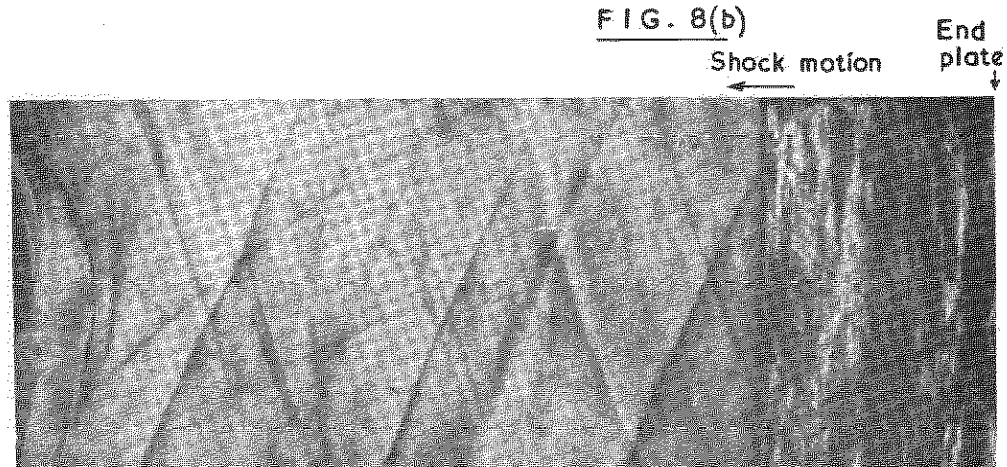
$$\left(\frac{P_{st'bl}}{P_3}\right) / P_{73} < 0.8$$

**FIG. 8 (a)**



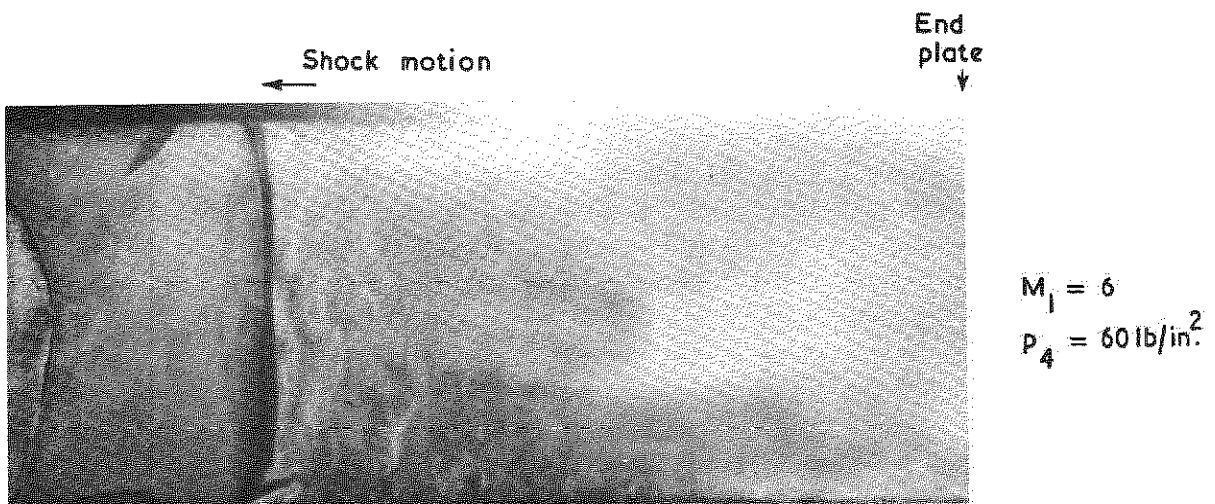
Determination of neutral stability Mach number for a Helium-Argon interface in a shock tube

FIG. 8(b)



Schlieren photographs of reflected shock waves in Argon  
at various Mach numbers. Helium driver gas

FIG. 8(c)



Bifurcated transmitted shock wave.  
Helium as driver gas, Argon as test gas.



**FIG. 9**

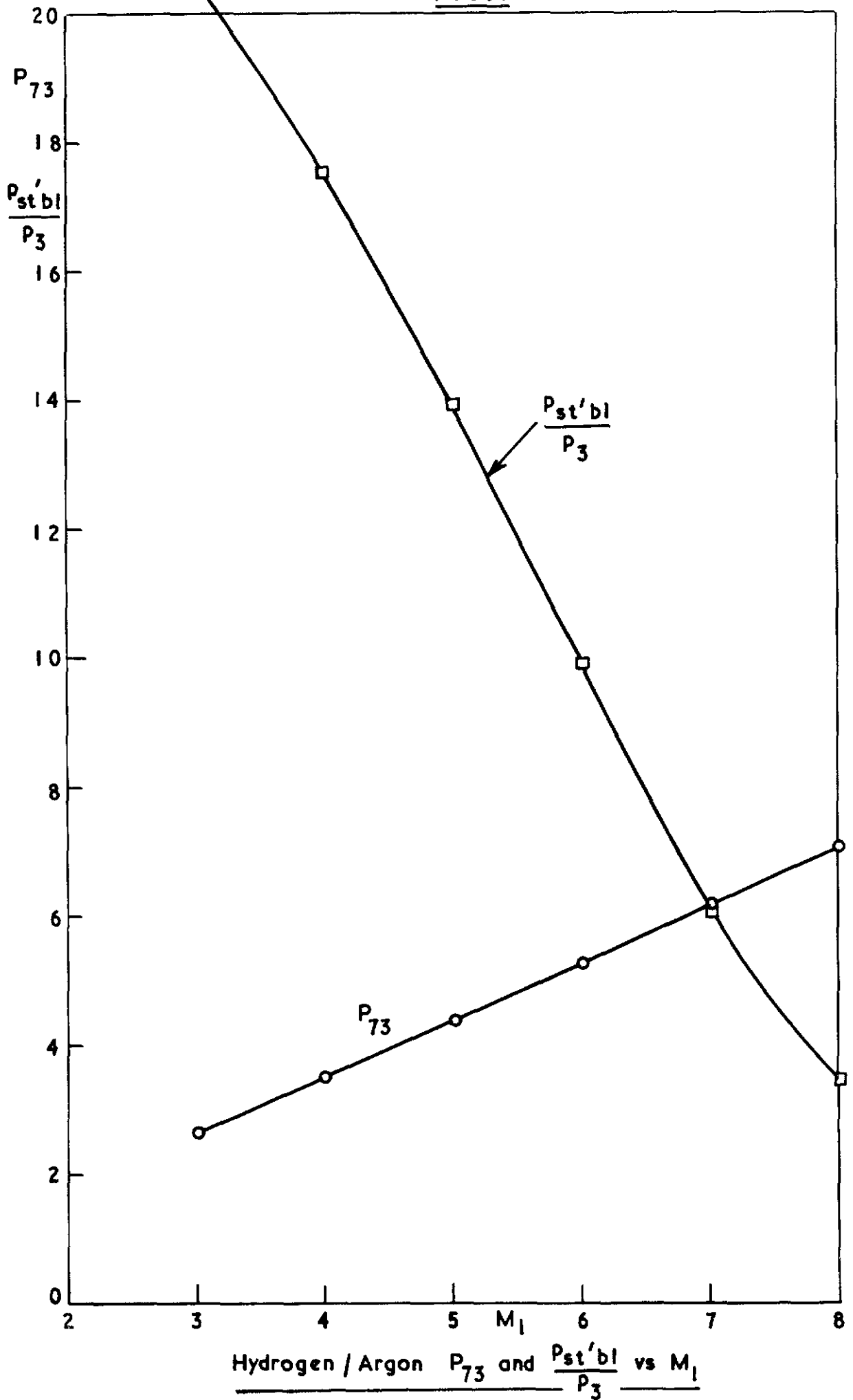
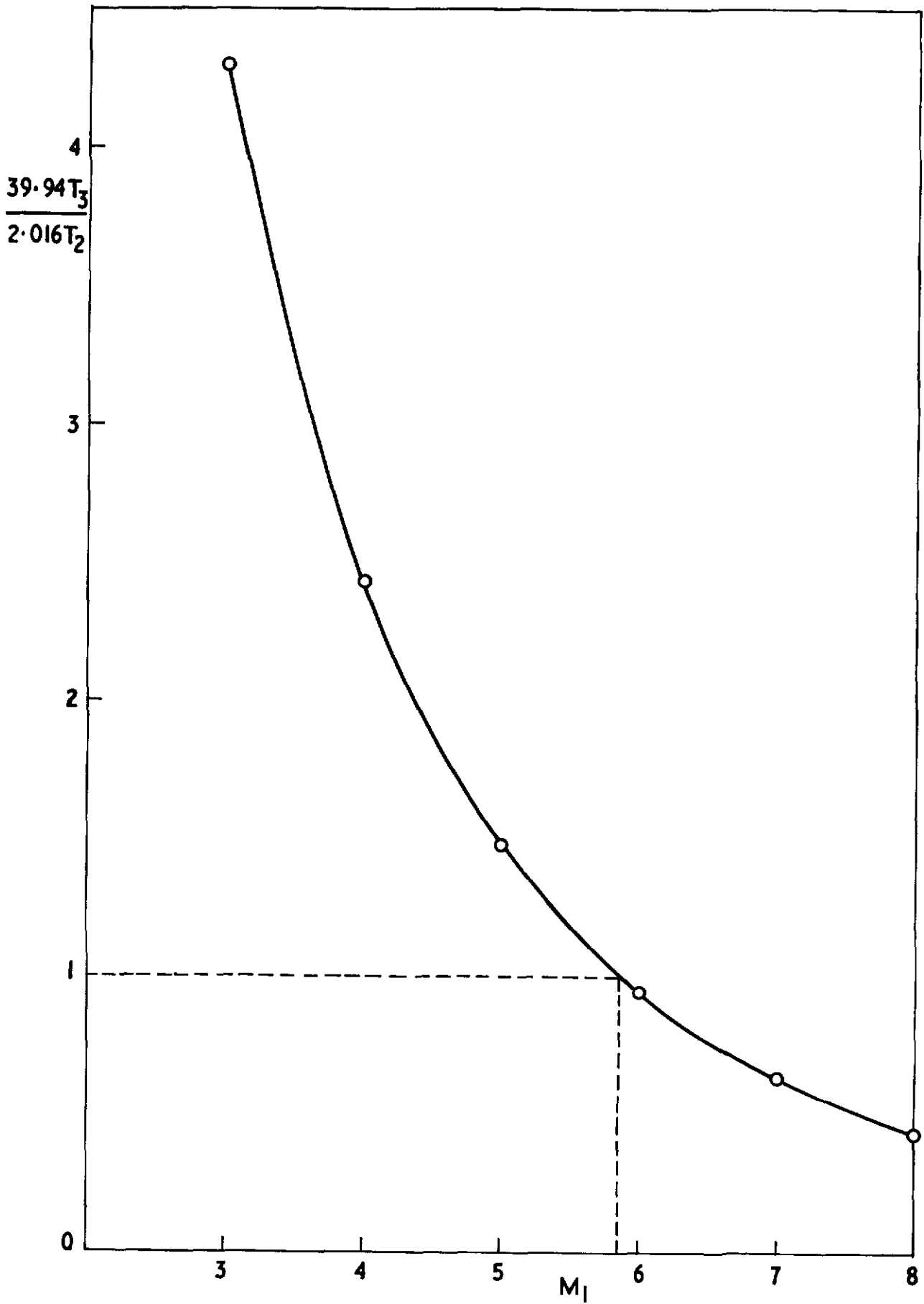


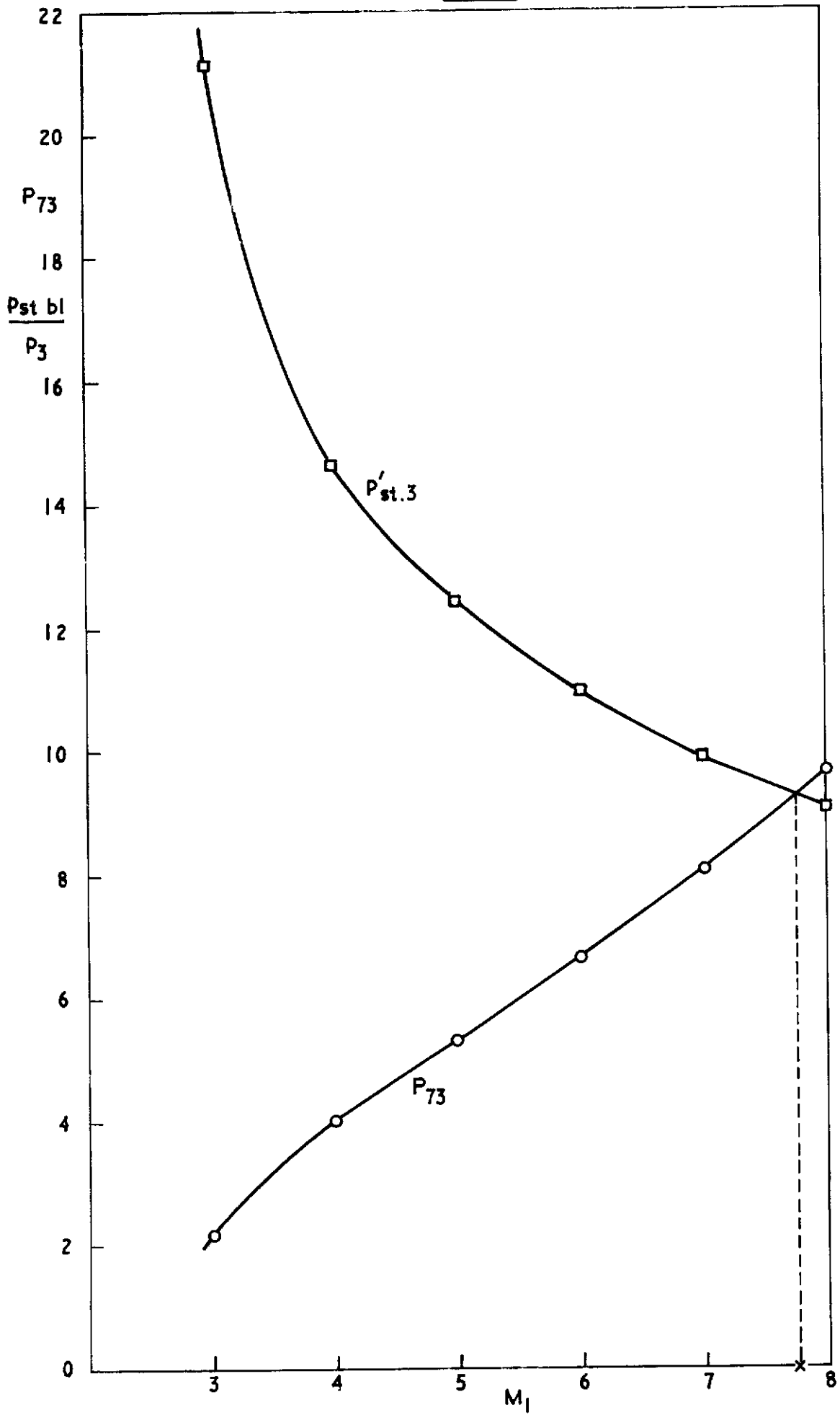
**FIG. 10**



Hydrogen / Argon

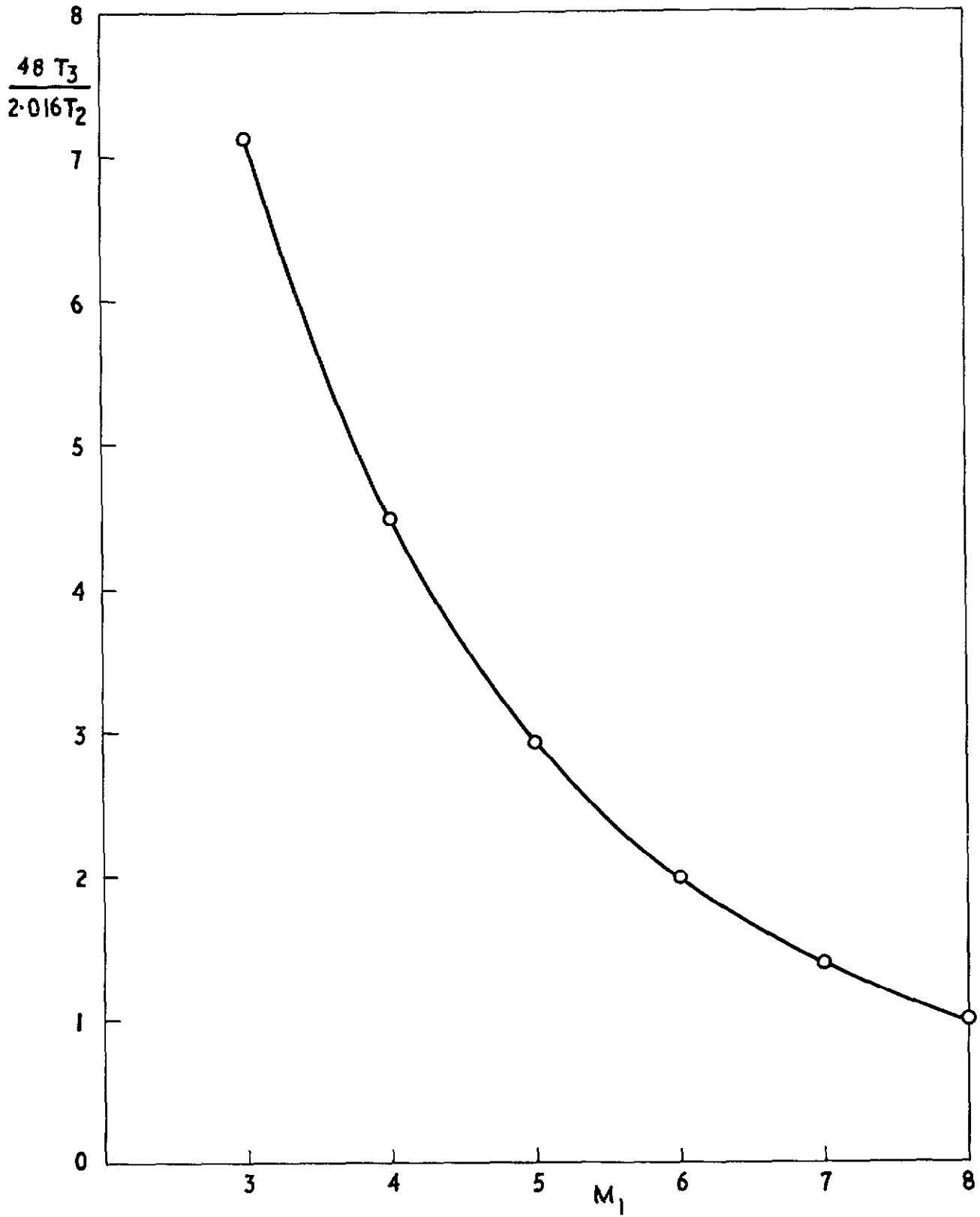
Determination of neutral stability Mach number

**FIG. 11**



Hydrogen / Carbon dioxide

FIG. 12



Hydrogen/Carbon dioxide

A.R.C. C.P. No. 881  
September, 1965  
Davies, L.

THE INTERACTION OF THE REFLECTED SHOCK WITH THE BOUNDARY LAYER IN A SHOCK TUBE AND ITS INFLUENCE ON THE DURATION OF HOT FLOW IN THE REFLECTED-SHOCK TUNNEL. PART II

Calculations are presented for the interaction of the shock transmitted through the contact surface with the boundary layer, using helium or hydrogen as the driver gases with nitrogen, argon and carbon dioxide as test gases. The relevance of the results to the cooling of the reservoir gas is discussed.

A.R.C. C.P. No. 881  
September, 1965  
Davies, L.

THE INTERACTION OF THE REFLECTED SHOCK WITH THE BOUNDARY LAYER IN A SHOCK TUBE AND ITS INFLUENCE ON THE DURATION OF HOT FLOW IN THE REFLECTED-SHOCK TUNNEL. PART II

Calculations are presented for the interaction of the shock transmitted through the contact surface with the boundary layer, using helium or hydrogen as the driver gases with nitrogen, argon and carbon dioxide as test gases. The relevance of the results to the cooling of the reservoir gas is discussed.

A.R.C. C.P. No. 881  
September, 1965  
Davies, L.

THE INTERACTION OF THE REFLECTED SHOCK WITH THE BOUNDARY LAYER IN A SHOCK TUBE AND ITS INFLUENCE ON THE DURATION OF HOT FLOW IN THE REFLECTED-SHOCK TUNNEL. PART II

Calculations are presented for the interaction of the shock transmitted through the contact surface with the boundary layer, using helium or hydrogen as the driver gases with nitrogen, argon and carbon dioxide as test gases. The relevance of the results to the cooling of the reservoir gas is discussed.

DETACHABLE ABSTRACT CARDS





C.P. No. 881

© *Crown copyright 1967*

Printed and published by

HER MAJESTY'S STATIONERY OFFICE

To be purchased from

49 High Holborn, London W C 1

423 Oxford Street, London W.1

13A Castle Street, Edinburgh 2

109 St Mary Street, Cardiff

Brazennose Street, Manchester 2

50 Fairfax Street, Bristol 1

35 Smallbrook, Ringway, Birmingham 5

80 Chichester Street, Belfast 1

or through any bookseller

*Printed in England*

C.P. No. 881